Enhanced Estimation of Rainfall From Opportunistic Microwave Satellite Signals

Sabina Angeloni, Elisa Adirosi, Fabiola Sapienza, Filippo Giannetti, Franco Francini, Lucio Magherini, Alessio Valgimigli, Attilio Vaccaro, Samantha Melani, Andrea Antonini, and Luca Baldini, *Senior Member, IEEE*

***Abstract*— Physical characteristics of precipitation, like temporal and spatial variability, jointly with coverage and costs of conventional meteorological devices for quantitative rainfall estimation (i.e., rain gauges, disdrometers, weather radars) make the precipitation monitoring a complex task. However, real-time rainfall maps are an important tool for many applications, dealing with environment, social activities, and business. Recently, the use of "opportunistic" methods to estimate rainfall has been investigated, highlighting the possibility to exploit inexpensive opportunities to augment information about precipitation. This article deals with smart low-noise blocks (SmartLNBs) converters, which are commercially available interactive digital video broadcasting (DVB) receivers designed to be used as bidirectional modems for commercial interactive TV applications. In the last few years, an algorithm that converts the SmartLNB raw data into attenuation values, from which the rainfall rate is obtained, has been developed and evaluated. The aim of this article is to describe the improvements of the rainfall estimation from SmartLNBs brought by significant changes in the data acquisition from SmartLNB and by algorithms' update. One year of data collected in Rome and Tuscany (Italy) are analyzed to test the performance of SmartLNB in estimating rainfall accumulation with respect to co-located rain gauges and disdrometer in the new configuration. Comparing SmartLNB and disdrometer data in Rome, we obtained root mean square error (RMSE) equal to 7.3 mm, normalized mean absolute error (NMAE) equal to 51%, with a correlation coefficient of 0.67, that can point out the maturity of the technique.**

***Index Terms*— Microwave (MW) satellite link, rain retrieval, rainfall attenuation.**

I. Introduction

INTEREST in precipitation measurements is growing for their impact on many disciplines and applications. Real-time rainfall monitoring is an important tool to be used for agriculture, water resource management, erosion, and energy production. It also plays a key role in short-term weather forecasting, and prediction of wildfire risk, early warning about flooding risk, and triggering of landslides.

The need for rainfall rate measurements is additionally motivated by the significant role that precipitation has in climate change, both in terms of intensity and spatial and temporal distribution. Recent years have witnessed a change in rainfall regimes almost everywhere [1], and the risk related to extreme precipitation is both significant and increasing.

Measuring the rain fallen can be challenging with conventional point measuring devices, due to the high temporal and spatial variability of precipitation, and requires a dense network of devices. Historically, rain gauges were the first devices used to provide local precipitation data, yielding accurate and direct measurement of rain accumulation (in mm). However, these devices collect data for the specific point of installation, not necessarily correlated with the surrounding areas. To improve the accuracy of spatial rainfall estimates obtained from rain gauges, it may be convenient to consider a network of rain gauges, which turns out to be inefficient due to its spatially inhomogeneous density [2]. Disdrometers are another category of point-measurement devices, yielding estimates of the drop size distribution (DSD) from which the corresponding rainfall rate is computed [3]. Some disdrometers also provide hydrometeors' fall velocity and size, allowing to distinguish different types of precipitation (rain, graupel, hail, or snow). However, similar to raingauges, they are point-devices with no capability to extract spatial rainfall distribution. On the other hand, weather radars can provide spatial features of precipitation with high spatial and temporal resolution, but the retrievals can be affected by many errors [4], [5].

Manuscript received 1 August 2023; revised 10 October 2023 and 4 December 2023; accepted 26 December 2023. Date of publication 1 January 2024; date of current version 17 January 2024. This work was supported in part by the Project Instruments for Intelligent Detection and Estimation of Rain for Agricultural Innovation (INSIDERAIN) through Tuscany Regional Administration (Italy), (18 December 2020), under Grant 21885; and in part by the Project Smart Control of the Climate Resilience in European Coastal Cities (SCORE) through the European Commission's Horizon 2020 Research and Innovation Program under Grant 101003534. *(Corresponding author: Elisa Adirosi.)*

Sabina Angeloni, Elisa Adirosi, and Luca Baldini are with the National Research Council of Italy, Institute of Atmospheric Sciences and Climate (CNR-ISAC), 00133 Rome, Italy (e-mail: sabina.angeloni@artov.isac.cnr.it; elisa.adirosi@artov.isac.cnr.it; l.baldini@isac.cnr.it).

Fabiola Sapienza and Filippo Giannetti are with the Department of Information Engineering, University of Pisa, 56122 Pisa, Italy (e-mail: fabiola.sapienza@ing.unipi.it; filippo.giannetti@unipi.it).

Franco Francini, Lucio Magherini, and Alessio Valgimigli are with ETG Srl, Manufacturer of Environmental Monitoring Systems, Florence, 50018 Scandicci, Italy (e-mail: f.francini@etgsrl.it; l.magherini@etgsrl.it; a.valgimigli@etgsrl.it).

Attilio Vaccaro is with MBI Srl, 56121 Pisa, Italy (e-mail: avaccaro@mbigroup.it).

Samantha Melani is with the National Research Council of Italy, Institute of BioEconomy (CNR-IBE), Florence, 50019 Sesto Fiorentino, Italy (e-mail: samantha.melani@cnr.it).

Andrea Antonini is with the Laboratory of Environmental Monitoring and Modeling for the Sustainable Development (LaMMA), Florence, 50019 Sesto Fiorentino, Italy (e-mail: antonini@lamma.toscana.it).

Digital Object Identifier 10.1109/TGRS.2023.3349100

Recently, the use of opportunistic signals to estimate rainfall has been investigated [6], aiming to expand the available measurement devices without adding new expensive infrastructures. The idea behind these new techniques is to exploit the existence of opportunistic microwave (MW) communication links distributed throughout the territory, even if installed for other purposes, and to measure the attenuation of the signal along the MW link caused by the presence of rain. Indeed, liquid and mixed-phase hydrometeors attenuate the power of the carrier signal and, subsequently, it is possible to convert a rain attenuation measurement into an instantaneous rainfall rate by means of specific inversion algorithms. Available MW links can be the terrestrial ones used for cellular communications and the Earth-to-satellite links used mainly for television signals broadcasting.

In the case of terrestrial radio links, dedicated pairs of antennas communicate with each other to transfer various types of data. Consequently, rain measurements accuracy is dependent on number, density and variety of directions of these paths [5], [7], [8], [9]. MW links of cellular communication networks guarantee a huge geographic capillarity which could improve the rainfall estimation at local scales. It is possible to obtain fairly accurate precipitation estimates relating to the area of interest where the receiver is located, since the MW path segment affected by rain is close to the terrestrial terminal.

In the case of satellite links, one or more receivers communicate with a telecommunication satellite. Higher density of receivers will enable higher accuracy and higher spatial resolution rainfall retrievals. More detailed description of the techniques using satellite-link signal attenuation measurements for estimating rainfall accumulation and to obtain rainfall maps can be found in [10], [11], [12], [13], [14], [15], and [16]. Both Earth-to-satellite and terrestrial links constitute complementary equipment for amplifying and improving the rain observation coverage of the territory.

The activities of INSIDERAIN (from September 2020 to December 2022) and NEFOCAST (from September 2016 to July 2019) projects, funded by the Tuscany Region Government (Italy), investigated and experimented in this research field. During NEFOCAST project a rain retrieval algorithm has been developed to obtain rainfall rate from commercial interactive digital video broadcasting (DVB) receivers called smart low-noise blocks (SmartLNBs) converters, and a platform to collect, process and store SmartLNB data, the NEFOCAST Service Center (NSC), was developed. Main results of the project are reported in [15] and [17]. During INSIDERAIN a new technique for the acquisition of SmartLNB data and several updates of the retrieval algorithm have been developed.

The purpose of this article is the description of the new INSIDERAIN retrievals, and its validation by comparison between SmartLNB retrievals with disdrometer and rain gauge data collected during 1-year experimental campaign at CNR-ISAC in Rome and in several sites in Tuscany. Compared to the NEFOCAST data analysis carried out in [17], the new acquisition mode and the upgraded algorithm allow SmartLNB to detect rather high rainfall rates, allowing the study of very intense precipitation phenomena. A further innovation compared to [17] is the presence, in Rome and Tuscany sites, of new smart rain gauges developed by ETG Srl, Italy, which are prototypes never used before, exploiting innovative techniques for measurement and diagnostic, that will be described and validated in the article.

This article is organized as follows. Section II deals with the description of the experimental deployment and the devices used in the campaign. Section III describes the rain retrieval algorithm highlighting its novelty with respect to the previous one, while Section IV explains the approach used in validation analysis. Section V shows the analysis of disdrometer and ETG rainfall data, with the aim of validating the ETG data and justifying the use of rain gauges as comparison devices in Tuscany. Section VI presents and discusses the main results obtained comparing the SmartLNB-based estimates with the conventional meteorological devices in Rome and in Tuscany. Finally, Section VII points out the main findings which are summarized and commented.

II. Experimental Setup

The SmartLNB used in this study is an innovative interactive satellite terminal produced by AYECKA Ltd., Israel (www.ayecka.com), which receives the Ku-band DVB satellite second generation (DVB-S2) downlink signal from EUTELSAT 10 A satellite, located at 10 °C East in the geostationary Earth orbit (GEO). All SmartLNB receivers are roughly oriented in the same direction and have the same inclination. The direction is approximately North–South as the longitude of the site area is between 10 °C and 12 °C East, while the satellite is in a geostationary orbit at 10 °C East longitude. The inclinations vary form 39.6 °C to 41.8 °C depending on the site. The length of the liquid path varies as function of the altitude of the zero degree isotherm. Measurements carried out on ground by the SmartLNBs are collected by the NSC via the return link through the same satellite. These terminals provide every 5 min the log of the instantaneous value of the signal-to-noise ratio (SNR), read every 10 s and averaged every 30 s and operate in Ku-band for the forward link. The data logger procedure running on the terminals has been modified to adopt a "store and forward" approach for data transmission: since the return link can be sometimes unavailable (e.g., during heavy rain events), if the terminal does not receive an acknowledgment of the transmission, data are locally stored to be sent when the link gets available again. In this way it is possible to improve monitoring continuity and avoid data losses. In this work, we deal with SmartLNBs installed in Rome and in several cities in Tuscany.

Rainfall data obtained from the SmartLNB in Rome (Fig. 1) are compared with those collected by the co-located disdrometer, which is a laser-based Thies Clima (TC) optical device manufactured by Adolf Thies GmbH & Company (www.thiesclima.com), Göttingen, Germany. The TC disdrometer provides information on size and fall velocity of each drop that falls into its measuring area, stores data over 1 min and groups particles into 22 and 20 classes of diameter size and fall velocity ranging from 0.125 to 8 mm and from 0.2 to

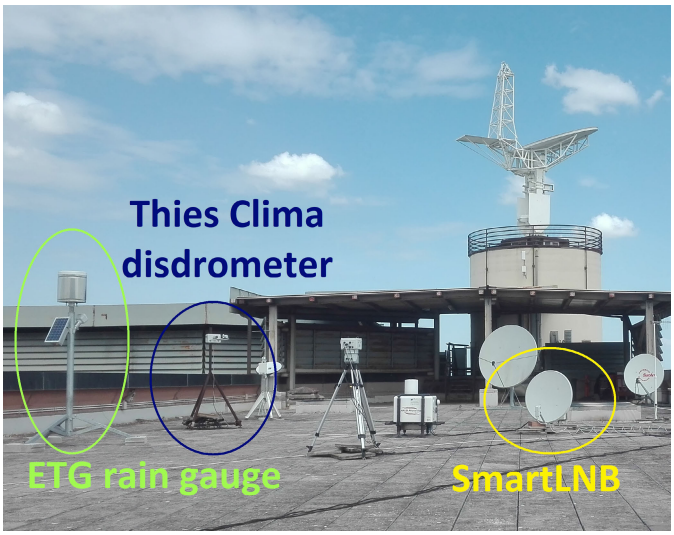

Fig. 1. Instrumentation at CNR-ISAC in Rome.

10 m·s^{-1}, respectively. Knowing the drop count matrix, the DSD (in m^{-3}·mm^{-1}) and the rain rate (in mm·h^{-1}) can be computed as

$$N(D_i) = \frac{1}{A\, v_i\, \Delta t\, \Delta D_i} \sum_{j=1}^{20} n_{i,j}$$

$$R = \frac{6\pi}{10^4 \varrho} \sum_i v_i\, D_i^3\, N(D_i)\, \Delta D_i$$

where D_i is the ith diameter class (mm), A is the measuring area of the disdrometer (45.6 cm^2), Δt is the time interval (60 s), ϱ is the water density (1 g·cm^{-3}), ΔD_i is the diameter class width (mm), $n_{i,j}$ is the number of particles detected in the ith diameter class and jth fall velocity class, and v_i is the fall velocity computed with the relation in [18]. A filter criterion is adopted to filter out the so-called spurious drops (such as the ones due to splashing and wind effects) and then mitigate the errors due to environmental factors. The drops with measured velocities outside ±50% of the fall velocity [18] are discarded.

In the sites of Tuscany, the measurements obtained by SmartLNBs are compared with those from co-located or nearby tipping bucket rain gauges, which provide, at discrete-time instants, measurements of the water quantity relative to a time interval with a resolution of 0.2 mm. In particular, the reference rain gauge in Florence is located in the same place as the SmartLNB, while in Massa it is located near the SmartLNB (GPS coordinates: 44.036599 N, 10.135836 E). In the sites in Pisa, the comparison device is a rain gauge by ETG Srl (www.etgsrl.it), Florence, Italy, located at 43.6678666667 N, 10.3477833333 E.

The new smart rain gauge developed by ETG introduces significant innovative aspects compared to the tipping bucket rain gauges currently on the market. Based on a 1000 cm^2 catching area and with 0.2 mm resolution, in accordance with WMO standards, the new rain gauge is equipped with three reed contacts positioned along the tilter's arc of movement (Fig. 2). The redundancy of the sensitive element will make possible to check the correct movement of the tipping bucket in the change of signal status (detachment from the rest position, overturning, arrival in the new rest position), so as to eliminate any erroneous readings due to any reed malfunctions. The new smart rain gauge has also been equipped with a group of self-diagnostic sensors (i.e., reeds positioned along the tilter's arc of movement, clogging, and temperature sensors) and an electronic processing unit able to obtain the correct values of the current quantity and precipitation intensity (cumulative precipitation, measured and compensated rainfall rate, moments of tilting), the reliability of the data detected, the possible presence of functional anomalies of the machine, and the need for maintenance (measurement system status, clogging status, and heating system status). A specific correction algorithm of the measured value as a function of the intensity, implemented on the firmware of the electronic unit, guarantees an error of less than 3% (Class A) in the entire measurement range.

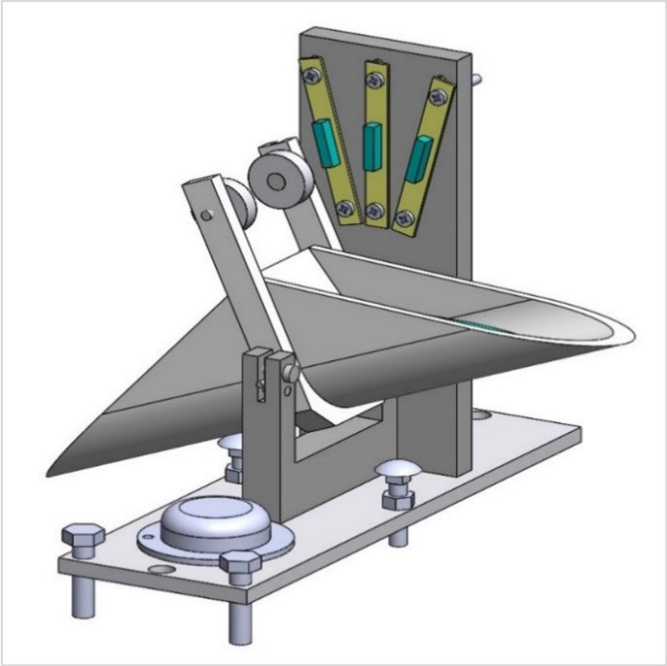

Fig. 2. Tilting bucket assembly in ETG rain gauge.

TABLE I
DATA AVAILABILITY TIMEFRAME FOR EACH TERMINAL

Device (site ID/name)	Data availability timeframe
SmartLNB (I)	01/01/2022 - 31/12/2022
TC disdrometer (I)	01/01/2022 - 31/12/2022
ETG rain gauge (I)	24/03/2022 - 31/12/2022
SmartLNB (IIA)	01/01/2022 - 01/08/2022
SmartLNB (IIB)	01/01/2022 - 10/07/2022
Rain gauge (IIB)	01/01/2022 - 07/07/2022
SmartLNB (IIC)	23/02/2022 - 31/12/2022
Rain gauge (Massa)	03/11/2022 - 31/12/2022
SmartLNB (IID)	21/04/2022 - 31/12/2022
SmartLNB (IIE)	01/01/2022 - 16/12/2022
ETG rain gauge (Pisa)	04/04/2022 - 31/12/2022

Table I shows the time intervals when rainfall data are available for each terminal. The distances between the sites where

TABLE II
SMARTLNB SITE COORDINATES AND DISTANCE FROM COMPARISON DEVICES

Site name	GPS coordinates	Distance between SmartLNB and comparison device [m]	Distance between comparison device and ground projection of slant path [m]
I – CNR-ISAC (RM)	41.840, 12.647	<10	<10
IIA – CNR-IBE (FI)	43.798, 11.192	4455	2045
IIB – Scuola di Musica (FI)	43.763, 11.165	<10	<10
IIC – Liceo 'Rossi' (MS)	44.035, 10.140	377	< 377
IID – UNIPI-DII (PI)	43.721, 10.384	6587	2757
IIE – Parrocchia S.B.A. (PI)	43.696, 10.428	7169	6369

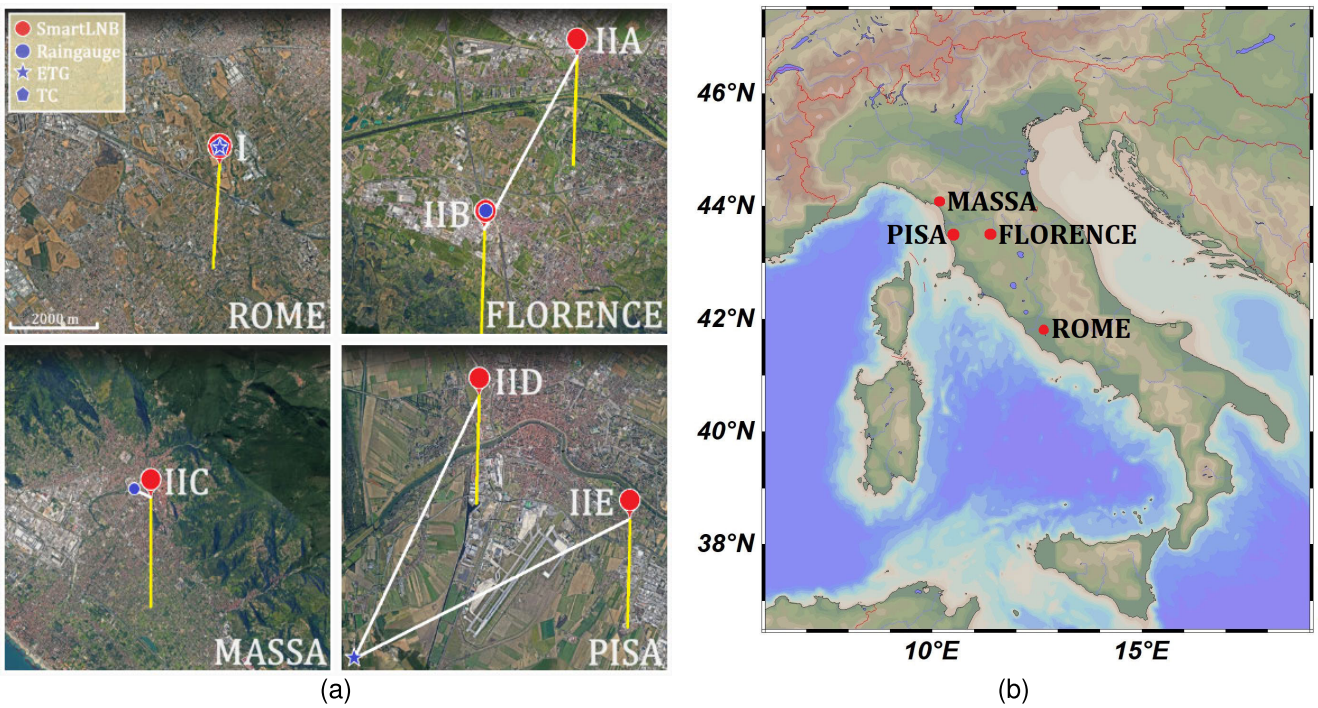

Fig. 3. (a) Locations of the instruments used in this study: SmartLNBs are indicated with red dots and reference devices with blue marks as in the legend. White lines indicate the distance between the instruments (third column in Table II), while yellow lines represent the ground projection of the slant path of SmartLNBs, assuming the 0 °C isotherm at 2 km height. (b) Location of the sites in Italy.

SmartLNBs are located and the ones of the corresponding comparison devices are signed in Table II, together with the distances between the reference instrument and ground projection of slant path, which represents the minimum measurement distance between rain gauge and SmartLNB (the abbreviations RM, FI, MS, and PI stand for Rome, Florence, Massa, and Pisa, respectively). Fig. 3 shows the locations of the instruments in the sites of Rome, Florence, Massa, and Pisa. Red dots represent SmartLNBs, while blue marks indicates the reference devices. White lines represent the ground distance between the instruments (third column in Table II), while yellow lines represent the ground projection of the slant path of SmartLNBs, assuming the 0 °C isotherm at 2 km height. It is possible to notice that shorter distances entail a tighter correlation between the two measurements, thus yielding better performance. In fact, as will be shown in the following, the error indices are minimal in Rome, Florence-Scuola di Musica, and Massa and greater in the other sites where rain gauges and SmartLNB are not co-located. In addition, the difference between the distances given in the last column of Table II for sites IID and IIE in Pisa clarifies why the performance of the SmartLNB at site IID is much better than that of the SmartLNB at site IIE, although the distances between rain gauge and SmartLNB are similar. Another important consideration is that the SmartLNBs used in the article detect precipitation roughly toward the south. For this reason, the rain gauges used as reference devices are located south of the SmartLNBs and as close as possible to the SmartLNB ground path. However, the direction of movement of the precipitation system, may affect the results and can be the subject of further analysis.

III. RAIN RETRIEVAL ALGORITHM

This section deals with the description of the upgraded algorithm which, together with the new acquisition mode, allow SmartLNB to detect higher rainfall rates, as shown in Section VI.

The opportunistic rain sensing method adopted in this study relies on the readings of the received signal strength (RSS) of MW downlinks from GEO telecommunication satellites. RRS

readings are thus the input data used for the computation of the attenuation introduced by the rain on the slanted wet path of the signal, which is ultimately converted into an estimate of the rainfall rate. Usually, RSS readings are provided by the receiving device itself. For instance, most commercial receivers for satellite broadcasting yield a measurement of the SNR, expressed as $\eta = E_s/N_0$, where E_s is the average RF energy per modulation symbol and N_0 is the one-sided power spectral density (PSD) of the overall noise affecting the received signal. The total additional attenuation A experienced by the MW signal during the rain event (wet condition) with respect to the pre-rain value (dry condition) can be obtained as [15]

$$A = (\eta^{\text{dry}}/\eta^{\text{wet}})(1-\xi)+\xi \tag{1}$$

where η^{dry} denotes the baseline level (suitably pre-calculated or prestored during clear-sky days), η^{wet} denotes the current RSS reading during precipitation, and ξ is a design parameter dependent on many noisy contributions as from cosmos, atmosphere, Earth, and the receiver's electronics (see [17, eq. (7)]). Different algorithms for the removal of other than rain components in satellite links have been developed, as in [6].

We assume then a stratiform precipitation, characterized by sharp separations between overlaying tropospheric layers. To this respect, ITU-R Rec. P.618 assumes a simple two-layer model, made of: 1) the attenuating liquid layer (LL) which starts from the ground level and extends up to the rain height h_R, containing only raindrops [23] and 2) the non-attenuating ice layer (IL), made of frozen dry particles above the rain height h_R. The LL-induced attenuation (1), suitably converted in dB (denoted as A[dB]), could be then plugged into the popular power law expressing the attenuation experienced by a MW signal due to rain, assumed uniform [10]

$$A[\text{dB}] = \alpha R^{\beta} L \tag{2}$$

where L is the length of the slanted wet radio path (in km), R is the rain rate (in mm·h^{-1}) within the LL, and α and β are frequency- and polarization-dependent empirical coefficients.

However, the approach in (2) reveals not accurate enough for rain estimation as it overlooks the phase transition in which the ice particles melt into raindrops. In our algorithm, we use therefore a more accurate three-layer model depicted in Fig. 4, wherein: 1) the LL is at the bottom, below the rain height h_R (we remark that here h_R represents the height of 100% liquid precipitation); 2) the IL is on top, above the 0 °C isotherm height h_0; and 3) an additional intermediate layer, named melting layer (ML) and containing a combination of melting ice and rain, is inserted between h_R and h_0. The attenuation introduced by ML on MW signals was characterized according to the outcomes of the studies available in [19] and it turned out to be dependent on the signal frequency and on the height within the ML. Equation (2), which describes the overall attenuation introduced along the wet portion of the slanted path, is then redefined as a function of both LL and ML parameters

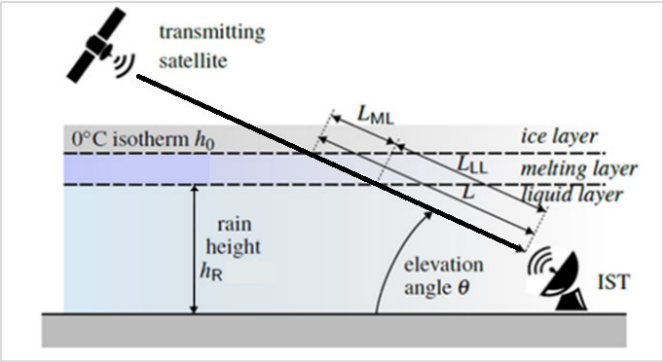

Fig. 4. Geometry of the satellite wet link (three-layer tropospheric model).

$$A[\text{dB}] = \alpha_{\text{ML}} R^{\beta_{\text{ML}}} L_{\text{ML}} + \alpha_{\text{LL}} R^{\beta_{\text{LL}}} L_{\text{LL}} \tag{3}$$

where the subscripts denote the tropospheric layer the parameters refer to. In particular, the coefficients α_{LL}, β_{LL}, α_{ML}, and β_{ML} and the lengths L_{LL} and L_{ML} of the wet radio path in the two layers can be derived as in [16]. Also, according to the literature, we implemented an upgraded version of the opportunistic rain rate estimator algorithm in which the contribution of the ML to the overall attenuation A is made significant only at low rain rates, as in [20].

Finally, the algorithm was further upgraded [21] so to take into account also the partial intersections of the slant path with randomly placed small-size rain cells, as in [10]. Further details cannot, however, be provided as the rain retrieval algorithm is protected by an international patent [22].

Due to implementation of the modifications above, the equation describing the overall attenuation A (i.e., concerning both LL and ML) to be solved in R turns out more involved than (2), being a function of both LL and ML parameters.

IV. Validation Approach

In this section, the approach used to evaluate the precipitation estimation from the SmartLNB is described.

A. Definition of Rain Events

The analysis is carried out on precipitation events occurred in 2022. The selection of the rain events is driven by disdrometer data in Rome and by rain gauges data in Tuscany. Taking into account the differences between the measurement methods of the two devices described above, it is appropriate to differentiate the definition of event. In Rome (respectively in Tuscany), a rain event is considered to last at least 60 (respectively 20) minutes with a maximum of 30 consecutive no-rain minutes. If the rainfall amount is less than 1.5 mm, the event is discarded. Furthermore, the 10 min preceding and following the event itself are also considered part of the event to avoid information loss deriving from any unlikely but possible time shifts of few minutes between the two devices, partially due to their different measuring principles. Information about the number of events N for each site and the average, maximum, and minimum values of the rainfall duration d are provided in Table III.

TABLE III
INFORMATION ON RAIN EVENTS AT EACH SITE

Site ID	**N**	**avg(d)** [min]	**max(d)** [min]	**min(d)** [min]
I	34	287	813	95
IIA	3	614	1334	186
IIB	11	406	1334	161
IIC	14	211	361	141
IID	18	257	513	108
IIE	18	262	513	108

B. Analysis of Detection Capability

The analysis of the SmartLNBs detection capability concerns the use of the contingency tables for each event and the calculation of the related indices: probability of detection (POD), false alarm ratio (FAR), and accuracy (ACC). The contingency table consists of the following parameters: the number of "hits" minutes H, when precipitation is detected by both the SmartLNB and the reference device (i.e., disdrometer or rain gauge); the number of "false alarm" minutes FA, when precipitation is detected by the SmartLNB but not by the reference device; the number of "missing" minutes M, when precipitation is detected by the reference device but not by the SmartLNB, and the number of "reject" minutes R, when both instruments do not detect precipitation.

The following statistical indices are calculated using the contingency tables. The POD index measures the probability that SmartLNB correctly detects precipitation when precipitation is actually present (i.e., detected by the reference device). The FAR index is calculated as the ratio between the number of no rain minutes wrongly categorized as rain minutes (false positives) and the total number of actual no rain minutes. The ACC index is how close rain measurements by SmartLNB are to their true value (measured by the reference device).

In formulas

$$\mathrm{POD} = \frac{H}{H+M}$$
$$\mathrm{FAR} = \frac{\mathrm{FA}}{H+\mathrm{FA}}$$
$$\mathrm{ACC} = \frac{H+R}{H+\mathrm{FA}+M+R}.$$

Contingency tables are defined only for SmartLNB and disdrometer comparison. In fact, they are of little use when using the rain gauge, as tipping bucket rain gauges do not detect low instantaneous rain rate values, unlike disdrometers. Tipping bucket rain gauges collect the number of tips that occur every minute. Each tip corresponds to an amount of water equivalent to 0.2 mm of rainfall, that is 12 mm·h^{-1} of rain rate. The disdrometer can measure even very low precipitation intensities (>0.1 mm·h^{-1}). Consequently, for low intensity precipitation the TC provides a measurement every minute and the rain gauge collects data only when a cumulated precipitation of 0.2 mm is reached. However, this behavior does not affect validation, which deals with total rainfall accumulation.

C. Analysis of Accuracy

The performance of the SmartLNB in providing accurate rainfall measurements is evaluated by comparing the rainfall accumulation (in mm) per event provided by SmartLNB with that measured by rain gauge or disdrometer. All the disdrometer/rain gauge or SmartLNB rainy minutes between the beginning and the end of a given event are considered to compute the total cumulated precipitation of that event. Graphical representation of the cumulative precipitation using scatterplot is provided. In addition, correlation coefficient, root mean square error (RMSE), normalized mean absolute error (NMAE), and normalized bias (NB) are calculated. The correlation coefficient measures the correlation between two variables, that is the degree to which they are linearly related. It assumes values in the range from -1 to $+1$, where ± 1 indicates the strongest possible agreement and 0 the strongest possible disagreement. RMSE is the standard deviation of the residuals and gives information on how concentrated the data is around the line of best fit.

In formulas

$$\mathrm{RMSE} = \sqrt{\overline{(Y-X)^2}}$$

where Y is the vector representing SmartLNB data and X is the vector of reference data. The NMAE is a normalization of the mean absolute error (MAE).

In formulas

$$\mathrm{MAE} = \frac{1}{N}\sum_{i=1}^{N}|Y_i - X_i|$$
$$\mathrm{NMAE} = \frac{\mathrm{MAE}}{\bar{Y}}.$$

N being the sample size.

The NB allows to evaluate the quality of the difference of the two datasets: negative NB values indicate an underestimation of SmartLNB with respect to the disdrometer or rain gauge, while positive NB indicate an overestimation of them. In formulas

$$\mathrm{NB} = \frac{\sum_{i=1}^{N} Y_i}{\sum_{i=1}^{N} X_i} - 1.$$

V. COMPARISON OF TC AND ETG RAINFALL DATA

In this section, precipitation measurements obtained from the TC disdrometer of CNR-ISAC in Rome are compared with those provided by the co-located ETG rain gauge. ETG rain gauge is a new smart prototype included in the measurement campaign to evaluate its performance. ETG is applying design and implementation changes to the rain gauge to improve its precipitation estimates. Therefore, the following analysis aims to validate the measurements of the ETG rain gauge and to justify the use of the disdrometer and the rain gauge as reference device for comparison with SmartLNB in Rome and in the Tuscany sites, respectively. The selection of the rain events is driven by the disdrometer data. The ETG rain gauge data are available from March 24, 2022. Events preceding this date are not analyzed. In the following, R_{cum} denotes the cumulated precipitation in mm. As an example,

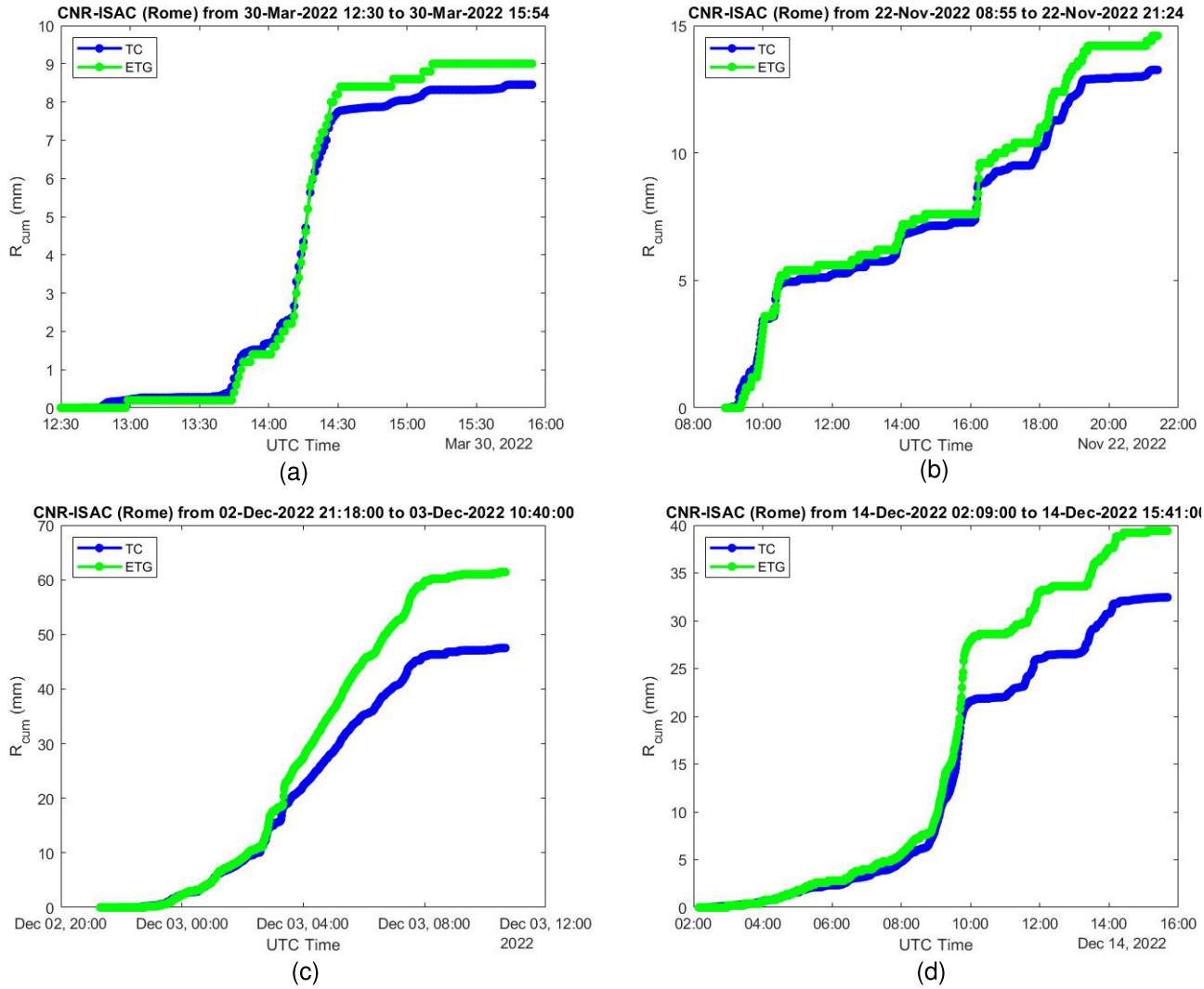

Fig. 5. Time series of cumulated precipitation from TC disdrometer and ETG rain gauge for four different rain events. (a) March 30, 2022 rain event. (b) November 22, 2022 rain event. (c) December 2, 2022 rain event. (d) December 14, 2022 rain event.

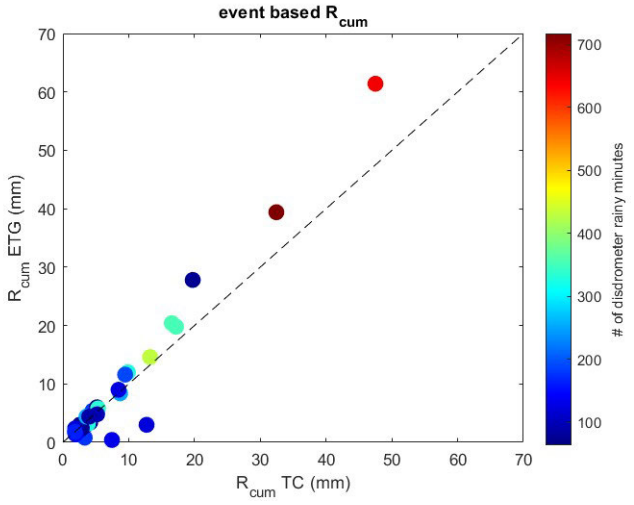

Fig. 6. Scatterplot between event-based cumulated precipitation estimated from TC disdrometer and ETG rain gauge in CNR-ISAC (Rome).

Fig. 5 shows the time series of the rainfall accumulation by TC disdrometer and ETG rain gauge for four different events.

TABLE IV
PERFORMANCE OF THE ETG RAIN GAUGE IN ESTIMATING RAINFALL ACCUMULATION WITH RESPECT TO TC DISDROMETER

Correlation	**RMSE** [mm]	**NMAE** [%]	**NB** [%]
0.98	4.2	25%	9 %

Fig. 6 shows the scatterplot between event-based cumulated precipitations estimated by TC disdrometer (x-axis) and ETG rain gauge (y-axis). The color bar represents the number of rainy minutes collected by the disdrometer during the events from March 24, 2022 to December 31, 2022.

The performance of the ETG rain gauge in estimating rainfall accumulation is illustrated in Table IV through the values of correlation coefficient, RMSE (in mm), NMAE (in %), and NB (in %) between cumulated precipitations measured by TC disdrometer and ETG rain gauge.

With few exceptions, the agreement between the data measured by the ETG rain gauge and those provided by the TC disdrometer is very good.

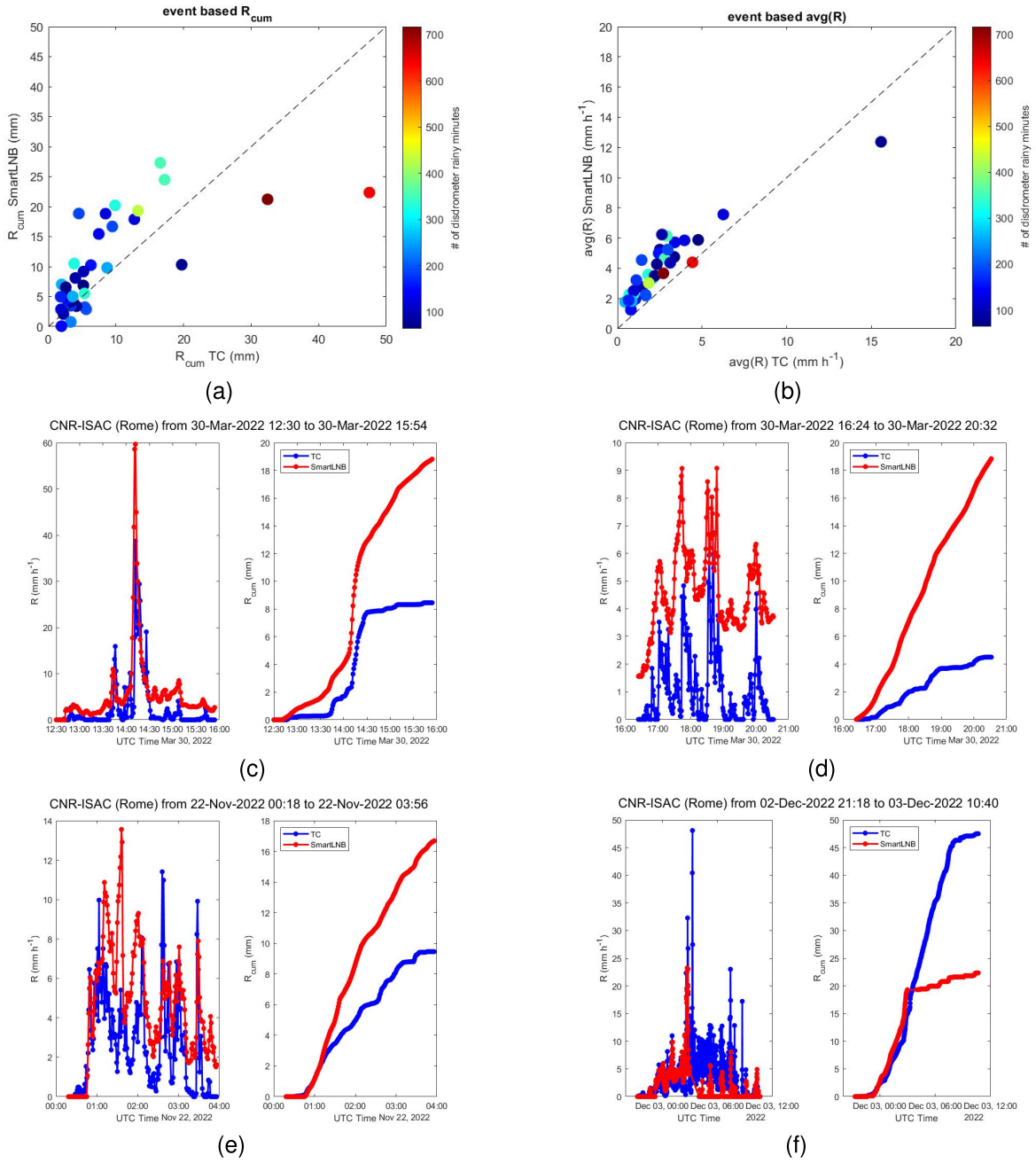

Fig. 7. CNR-ISAC (Rome). (a) Scatterplot between event-based cumulated precipitation from TC disdrometer and SmartLNB. (b) Scatterplot between event-based mean value of rain rate from TC disdrometer and SmartLNB. (c)–(f) Time series of cumulated precipitation from TC disdrometer and SmartLNB.

TABLE V

CONTINGENCY TABLE PROCESSED ON ALL RAINY EVENTS FOR DETECTION ANALYSIS OF SMARTLNB WITH RESPECT TO TC DISDROMETER IN ROME

Hits [min]	**False Alarm** [min]	**Missing** [min]	**Reject** [min]
4527	777	2396	1604

TABLE VI

STATISTICAL INDICES OBTAINED BY CONTINGENCY TABLES OF SMARTLNB WITH RESPECT TO TC DISDROMETER IN ROME

POD [%]	**FAR** [%]	**ACC** [%]
65%	15%	66%

VI. EVALUATION OF THE PRECIPITATION ESTIMATION FROM SMARTLNB

In this section, we compare the SmartLNB rainfall retrievals with the data provided by the TC disdrometer in Rome and the rain gauges in Tuscany.

A. Validation in Rome

The first step deals with the analysis of the SmartLNB performance in detecting rainy events. Table V shows the contingency table obtained considering all the rainy events. The high number of "missing" minutes is due to the fact

TABLE VII
PERFORMANCE OF THE SMARTLNB IN ESTIMATING RAINFALL ACCUMULATION WITH RESPECT TO TC DISDROMETER

Correlation	**RMSE** [mm]	**NMAE** [%]	**NB** [%]
0.67	7.3	51%	23%

that the disdrometer is able to detect very low rainfall data (>0.1 mm·h^{-1}), unlike the SmartLNB. Indeed, the average value of rain rate provided by the disdrometer in "missing" minutes is equal to 0.7 mm·h^{-1}.

The statistical indices POD, FAR, and ACC related to contingency tables are shown in Table VI.

As second step the SmartLNB-based cumulated precipitation obtained in each event is compared with that obtained from the TC disdrometer, to evaluate the SmartLNB performance in providing accurate rainfall measurements. Fig. 7(a) shows the scatterplot between event-based cumulated precipitation estimated by TC disdrometer (x-axis) and SmartLNB (y-axis). The color bar represents the number of rainy minutes collected by the disdrometer during the event.

Table VII shows the values of correlation coefficient, RMSE (in mm), NMAE (in %), and NB (in %) between cumulated precipitations measured by TC disdrometer and SmartLNB.

An overestimation of the SmartLNB retrieval with respect to the disdrometer measurement is observed and is mainly associated with two phenomena. For some events, as the ones shown in Fig. 7(d) and (e), there is a small bias between the two time series of instantaneous rainfall rate (although the agreement between the trends is good), which causes a high difference in terms of cumulated precipitation. The latter bias can be due to a small error in the definition of the Es/N0 reference values in the SmartLNB retrieval algorithm.

The second aspect is that sometimes the SmartLNB overestimates the values of very intense rain rate peaks [Fig. 7(c)].

Although a possible overestimation of the peaks, it is worth noting that the SmartLNB is able to detect high precipitation values, obtaining an improvement compared to the analysis carried out in [17]. Fig. 7(f) shows an event during which the rain rate peak of 48.1 mm·h^{-1} measured by the disdrometer is not detected by SmartLNB. However, this is a rare situation, probably due to a saturation phenomenon.

The overestimation of rainfall peaks, although time localized, and the small bias can lead to a significant overestimation of the average value of the rainfall rate R per event. Fig. 7(b) shows the scatterplot between event-based mean value of R obtained by TC disdrometer data (x-axis) and SmartLNB ones (y-axis). The color bar represents the number of rainy minutes collected by the disdrometer during the event.

Finally, to summarize the main behavior of the SmartLNB retrievals algorithm, with respect to the disdrometer, Fig. 8 shows a bar plot which highlights the total accumulation rainfall (calculated on all the events) measured by the two instruments for different precipitation intensity classes (obtained by the disdrometer). The underestimation when R varies between 0 and 2 mm·h^{-1} is caused by the non-detection of low rain intensities by SmartLNB. In general,

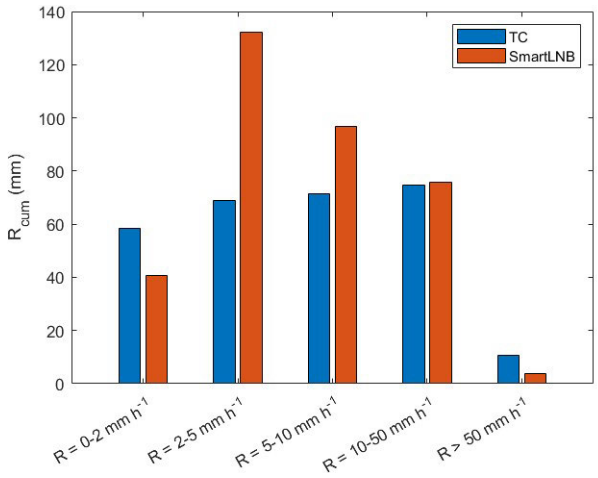

Fig. 8. Bar plot of the total accumulation rainfall as the rainfall rate (measured by TC disdrometer) varies.

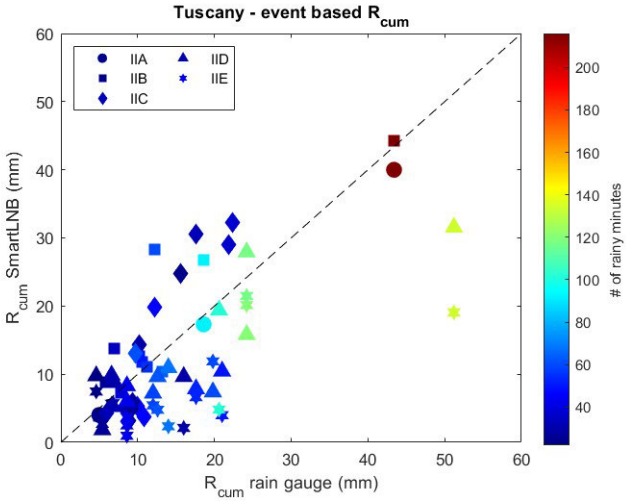

Fig. 9. Scatterplot between event-based cumulated precipitation from rain gauges and SmartLNBs in Tuscany.

the SmartLNB overestimates the precipitation data (especially for medium intensities) and is able to detect very high rainfall rate values.

B. Validation in Tuscany

The SmartLNB-based cumulated precipitation obtained in each event is compared with that obtained from the rain gauge, at each selected site in Tuscany. The performances of the SmartLNBs in providing accurate rainfall measurements are evaluated and illustrated in Fig. 9 and Table VIII.

Fig. 9 shows the scatterplot between event-based cumulated precipitations estimated by rain gauge (x-axis) and SmartLNB (y-axis), for each site in Tuscany (as described in the legend).

Table VIII shows the error values, obtained for sites where it is possible to compare at least ten events, while the last row of the table shows the results obtained considering the complete set of data from all sites in Tuscany.

The correlation coefficient varies among the different sites, ranging between 0.50 and 0.92, with an overall performance of 0.70. This is due to the inhomogeneity of the data: in fact, the events analyzed refer to different areas and time periods,

TABLE VIII
PERFORMANCE OF THE SMARTLNB IN ESTIMATING RAINFALL ACCUMULATION WITH RESPECT TO RAIN GAUGE

Site ID	Correlation	RMSE [mm]	NMAE [%]	NB [%]
IIB	0.89	6.0	24%	23%
IIC	0.92	6.7	43%	14%
IID	0.83	7.4	49%	-26%
IIE	0.50	14.9	157%	-61%
All sites	0.70	8.3	50%	-18%

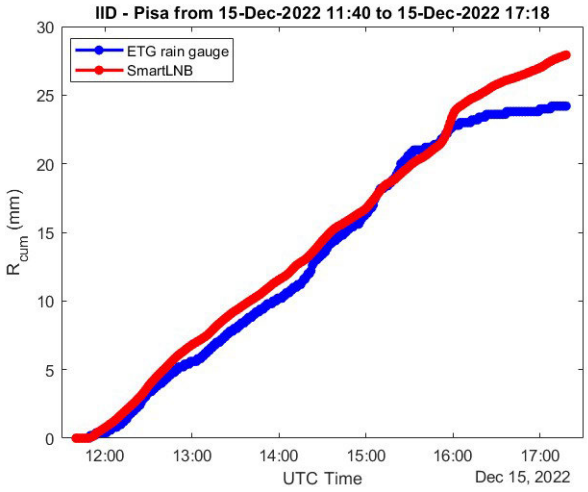

Fig. 10. Time series of cumulated precipitation by ETG rain gauge in Pisa and SmartLNB in site IID for the December 15, 2022 rain event.

according to the availability of the data itself. Based on RMSE and NMAE, the SmartLNB IIB has the best performance (6.0 mm and 24%, respectively). In terms of bias, sites IIB and IIC have positive values (23% and 14%, respectively), while IID and IIE have negative NB values (−26% and −61%, respectively). However, the overall bias is −18%. The SmartLNB IIE in Pisa has the worst performance in terms of the error indices considered. It is possible to notice that shorter distances correspond to better performance. In fact, a comparison of Tables I and VIII yields that the error indices are minimal IIB and IIC and greater in the other sites where rain gauges and SmartLNB are not co-located. In addition, the difference between the distances given in the last column of Table I for sites IID and IIE in Pisa clarifies why the performance of the SmartLNB at site IID is much better than that of the SmartLNB at site IIE, although the distances between rain gauge and SmartLNB are similar.

Fig. 10 shows an example of good agreement between the time series of the rainfall accumulation by SmartLNB and ETG rain gauge, related to the site IID in Pisa.

VII. CONCLUSION

Recently, the use of "opportunistic" methods to estimate rainfall has been investigated, aiming to augment precipitation measurements by expanding available devices without adding new infrastructures. The idea behind these new techniques is to exploit the existence of opportunistic MW communication links distributed throughout the territory, even if installed for other purposes, and to measure the attenuation experienced by the signals as a consequence of the presence of liquid and mixed precipitation along the receiver-satellite path.

In this context, two projects funded by the Tuscany Region Government (Italy), NEFOCAST and INSIDERAIN, have been carried out with the purpose of developing and evaluating a rain retrieval algorithm to obtain rainfall rate from interactive domestic devices. In particular, INSIDERAIN is a follow-up of the NEFOCAST project and provides significant changes with respect to NEFOCAST retrievals.

To validate the new INSIDERAIN retrievals a 1-year field campaign was conducted at CNR-ISAC in Rome and in several sites in Tuscany. Comparing SmartLNB with disdrometer and rain gauge data we found that the new acquisition mode and the upgraded algorithm allow SmartLNB to detect higher rainfall rates, ensuring the study of intense precipitation phenomena, i.e., up to about 100 mm·h^{-1}. The latter is an improvement compared to the NEFOCAST analysis carried out in [17]. A further innovation to [17] is the presence, in Rome and Tuscany sites, of new smart rain gauges developed by ETG Srl, Italy, which are prototypes never used before. The comparison of the ETG and disdrometer measurements results in a correlation coefficient of 0.98 and NMAE equal to 25%, highlighting the very good performance of the new device.

We found that in terms of event cumulated precipitation values the agreement between SmartLNB and disdrometer in Rome is good, i.e., NMAE (RMSE) equal to 51% (7.3 mm) and a bias of 23%. However, the SmartLNB overestimates the precipitation intensities (especially for medium values, i.e., around 10 and 20 mm·h^{-1}). The same comparison analysis between rain gauges and SmartLNBs in Tuscany yields to similar error values, i.e., an overall NMAE (RMSE) equal to 50% (8.3 mm). Regarding the sites in Tuscany the resulting bias is positive in some cases and negative in others. Similar results have been obtained in [17] where lower precipitation intensity events have been analyzed.

Although the technology covered by this article has been tested in two different projects obtaining good comparison results, it is not yet mature for operation. Analysis over longer periods and comparisons with multiple rain gauges arranged along the satellite link are necessary to study the effects of different acquisition geometry on the results. In [11], an ensemble Kalman filter (EnKF)-based method is developed to dynamically generate gridded rainfall fields, assimilating precipitation from MW links.

ACKNOWLEDGMENT

The authors acknowledge ARPA Piemonte (Dr. R. Cremonini, Dr. R. Bechini, and Dr. V. Campana) who provided the disdrometer for the Rome site.

REFERENCES

[1] M. Collins et al., "Long-term climate change: Projections, commitments and irreversibility," *Climate Change 2013: The Physical Science Basis*, T. F. Stocker et al., Eds. Cambridge, U.K.: Cambridge Univ. Press, 2013, pp. 1029–1136.

[2] C. Kidd et al., "So, how much of the Earth's surface is covered by rain gauges?" *Bull. Amer. Meteorolog. Soc.*, vol. 98, no. 1, pp. 69–78, Jan. 2017.
[3] G. Kathiravelu, T. Lucke, and P. Nichols, "Rain drop measurement techniques: A review," *Water*, vol. 8, no. 1, p. 29, Jan. 2016.
[4] S. Sebastianelli, F. Russo, F. Napolitano, and L. Baldini, "On precipitation measurements collected by a weather radar and a rain gauge network," *Natural Hazards Earth Syst. Sci.*, vol. 13, no. 3, pp. 605–623, Mar. 2013, doi: 10.5194/nhess-13-605-2013.
[5] R. M. Rauber and S. W. Nesbitt, *Radar Meteorology*. Hoboken, NJ, USA: Wiley, 2018, doi: 10.1002/9781118432662.
[6] J. Ostrometzky, G. Rafalovich, B. Kagan, and H. Messer, "Stand-alone, affordable IoT satellite terminals and their opportunistic use for rain monitoring," *IEEE Internet Things Mag.*, vol. 5, no. 4, pp. 100–105, Dec. 2022, doi: 10.1109/IOTM.001.2200166.
[7] H. Leijnse, R. Uijlenhoet, and J. N. M. Stricker, "Rainfall measurement using radio links from cellular communication networks," *Water Resour. Res.*, vol. 43, no. 3, Mar. 2007, Art. no. W03201, doi: 10.1029/2006WR005631.
[8] B. Lian, Z. Wei, X. Sun, Z. Li, and J. Zhao, "A review on rainfall measurement based on commercial microwave links in wireless cellular networks," *Sensors*, vol. 22, no. 12, p. 4395, Jun. 2022, doi: 10.3390/s22124395.
[9] G. Roversi, P. P. Alberoni, A. Fornasiero, and F. Porcù, "Commercial microwave links as a tool for operational rainfall monitoring in Northern Italy," *Atmos. Meas. Techn.*, vol. 13, no. 11, pp. 5779–5797, Oct. 2020, doi: 10.5194/amt-13-5779-2020.
[10] F. Giannetti and R. Reggiannini, "Opportunistic rain rate estimation from measurements of satellite downlink attenuation: A survey," *Sensors*, vol. 21, no. 17, p. 5872, Aug. 2021.
[11] A. Ortolani, F. Caparrini, S. Melani, L. Baldini, and F. Giannetti, "An EnKF-based method to produce rainfall maps from simulated satellite-to-ground MW-link signal attenuation," *J. Hydrometeorol.*, vol. 22, pp. 1333–1350, Mar. 2021.
[12] L. Barthès and C. Mallet, "Rainfall measurement from the opportunistic use of an Earth-space link in the Ku band," *Atmos. Meas. Techn.*, vol. 6, no. 8, pp. 2181–2193, Aug. 2013.
[13] C. H. Arslan, K. Aydin, J. V. Urbina, and L. Dyrud, "Satellite-link attenuation measurement technique for estimating rainfall accumulation," *IEEE Trans. Geosci. Remote Sens.*, vol. 56, no. 2, pp. 681–693, Feb. 2018.
[14] M. Colli et al., "A field assessment of a rain estimation system based on satellite-to-Earth microwave links," *IEEE Trans. Geosci. Remote Sens.*, vol. 57, no. 5, pp. 2864–2875, May 2019.
[15] F. Giannetti et al., "Real-time rain rate evaluation via satellite downlink signal attenuation measurement," *Sensors*, vol. 17, no. 8, p. 1864, Aug. 2017.
[16] F. Giannetti, M. Moretti, R. Reggiannini, and A. Vaccaro, "The NEFOCAST system for detection and estimation of rainfall fields by the opportunistic use of broadcast satellite signals," *IEEE Aerosp. Electron. Syst. Mag.*, vol. 34, no. 6, pp. 16–27, Jun. 2019.
[17] E. Adirosi et al., "Evaluation of rainfall estimation derived from commercial interactive DVB receivers using disdrometer, rain gauge, and weather radar," *IEEE Trans. Geosci. Remote Sens.*, vol. 59, no. 11, pp. 8978–8991, Nov. 2021.
[18] D. Atlas, R. C. Srivastava, and R. S. Sekhon, "Doppler radar characteristics of precipitation at vertical incidence," *Rev. Geophys.*, vol. 11, no. 1, pp. 1–35, Feb. 1973.
[19] A. Dissanayake, J. Allnutt, and F. Haidara, "A prediction model that combines rain attenuation and other propagation impairments along Earth-satellite paths," *IEEE Trans. Antennas Propag.*, vol. 45, no. 10, pp. 1546–1558, 1997.
[20] F. Sapienza, G. Bacci, F. Giannetti, A. Vaccaro, and V. Lottici, "Tropospheric propagation modeling for opportunistic rain sensing using current and future broadcast and broadband satellites," in *Proc. 35th Gen. Assem. Sci. Symp. Int. Union Radio Sci. (URSI GASS)*, Sapporo, Japan, Aug. 2023, pp. 1–4, doi: 10.23919/URSIGASS57860.2023.10265526.
[21] G. H. Bryant, I. Adimula, C. Riva, and G. Brussaard, "Rain attenuation statistics from rain cell diameters and heights," *Int. J. Satell. Commun.*, vol. 19, no. 3, pp. 263–283, May 2001, doi: 10.1002/sat.673.
[22] F. Giannetti, R. Reggianini, M. Moretti, and A. Colicelli, "Method for estimating the presence of rain," Int. Patent Appl. PCT/IB 2021 056 594, Jul. 20, 2021.
[23] *Propagation Data and Prediction Methods Required for the Design of Earth-Space Telecommunication Systems*, document ITU-R P.618-13, Dec. 2017.

Sabina Angeloni received the master's degree (cum laude) in mathematics from the Sapienza University of Rome, Rome, Italy, in 2018, and the Ph.D. degree (cum laude) in mathematical analysis from Roma Tre University, Rome, in 2022.

She is a Research Fellow with the Institute of Atmospheric Sciences and Climate, National Research Council (CNR-ISAC), Rome. She has been involved in the validation campaign of the INSIDERAIN project and she is currently involved in the SCORE project.

Elisa Adirosi received the master's degree in environmental engineering and the Ph.D. degree in environmental and hydraulic engineering from the Sapienza University of Rome, Rome, Italy, in 2009 and 2015, respectively.

She has been a Visiting Scientist with Goddard Space Flight Center, NASA, Greenbelt, MD, USA, and a Researcher with the Institute of Atmospheric Sciences and Climate, National Research Council (CNR-ISAC), Rome. She develops innovative mathematical methods to analyze disdrometer data and investigates the characteristics of simulated and observed drop size distributions to improve precipitation retrieval from remote sensing measurements. She has been involved in the NEFOCAST and INSIDERAIN projects and she is currently involved in the SCORE project.

Fabiola Sapienza received the master's degree in telecommunication engineering from the University of Pisa, Pisa, Italy, in July 2020.

Since December 2020, she has been a Research Fellow with the Department of Information Engineering, University of Pisa, with experience in the analysis and processing of satellite signals. She has been involved in the development and calibration of the rainfall rate estimation algorithm in the INSIDERAIN project and she is currently involved in the SCORE project.

Filippo Giannetti is a Professor of telecommunications at the Department of Information Engineering of the University of Pisa, Pisa, Italy. He worked on several international projects (EU's FP7 and H2020, ESA) and authored more than 170 journal and conference papers. He is a co-inventor of several patents, including an innovative technique for rainfall estimation based on opportunistic measurement of satellite signal strength. His main research interests concern digital signal processing, wireless communications, satellite systems, radiopropagation, and rainfall measurement.

Dr. Giannetti is a member of the Editorial Board of EURASIP Journal on Wireless Communications and Networking.

Franco Francini is the Technical Manager of ETG Srl, Florence, Italy, with over 50 years of experience in the sector, and coordinates the work group in the management of research and development projects. Graduated in electrical engineering, he carried out the functions of technical management at headquarters and in the field, personnel management, and organization of the work group; he coordinated the implementation of the most important projects thanks to the skills acquired and matured in the field of electronic and telecommunications design.

Lucio Magherini has been a Commercial Technician at ETG Srl, Florence, Italy, for over five years. He has 25 years of experience in the company and the environmental monitoring sector, first in the Technical Assistance Department as Head of the Maintenance Department and Services, and subsequently in the commercial management of orders and technical and economic design of solutions and proposals, also relating to calls for regional and national funding.

Alessio Valgimigli received the degree in telecommunications engineering from the University of Florence, Florence, Italy, in 2005.

He is the Research and Development Manager of ETG Srl. He has over 20 years of experience in the hardware, software, and firmware design of environmental monitoring systems. Through the management of internal and external resources, he coordinates the development of hardware and software products thanks to specific skills in hardware design and Javascript/C/PHP/Suite Yocto Project/Wireless Networking/HTML, Javascript and CSS/Linux Embedded and Yocto Project Training.

Attilio Vaccaro is the Director of Innovation in MBI Srl, where he deals with research and development activities in the domain of satellite communications, the Internet of Things, smart sensing technologies, and hybrid communications. Involved in several public research activities (e.g., ESA and EU cofunded projects), coordinator for the NEFOCAST and INSIDERAIN projects of Tuscany Region. Innovation manager in the SCORE project.

Samantha Melani received the master's degree in physics and the Ph.D. degree in physical modeling for environmental protection from the University of Bologna, Bologna, Italy, in 1999 and 2006, respectively.

She is a Researcher with the Institute of BioEconomy, National Research Council (CNR-IBE), Florence, Italy, part-time assigned to Consorzio LaMMA, Florence, Italy. She has been involved in the NEFOCAST and INSIDERAIN (as Scientific coordinator) projects. Her scientific interest focuses on atmospheric science, in particular dealing with atmospheric remote sensing of cloud systems using satellite and radar techniques, cloud physics studies of severe storms, and validation techniques for heterogeneous data.

Andrea Antonini received the Laurea degree in electronic engineering from the University of Florence, Florence, Italy, in 2002, and the Ph.D. degree in geoinformation engineering from the University of Tor Vergata, Rome, Italy, in 2013. Since 2011, he has been formally a Researcher at LAMMA Consortium, Florence, Italy. He has been involved in NEFOCAST and INSIDERAIN projects. The main research interests are meteorological applications of sensors and remote sensing techniques, spanning from radar and satellite to GNSS meteorology and ground-based observations.

Luca Baldini (Senior Member, IEEE), received the Laurea degree in electrical engineering and the Ph.D. degree in methods and technologies for environmental monitoring from the University of Florence, Florence, Italy, in 1988 and 1994, respectively.

From 1994 to 2001, he was a Teacher of remote sensing systems with the University of Siena, Siena, Italy, and a Teacher of Signal Theory with the University of Florence, in 1996. From 1995 to 2001, he worked as an Independent Consultant, in Italy. In 2001, he joined the Institute of Atmospheric Sciences and Climate of the National Research Council of Italy (CNR-ISAC), Rome, Italy as a Researcher, where he is a In Charge of research on precipitation measurements, particularly on radar polarimetry applied to quantitative precipitation estimation, characterization of precipitation microphysics, and ground validation of precipitation measurements from satellites. He has been involved in the NEFOCAST and INSIDERAIN projects and is involved in the EU H2020 SCORE project.

Open Access funding provided by 'Consiglio Nazionale delle Ricerche-CARI-CARE-ITALY'
within the CRUI CARE Agreement